

# Reaction of DMS and HOBr as a Sink for Marine DMS and an Inhibitor of Bromoform Formation

Emanuel Müller, Urs von Gunten, Sylvain Bouchet, Boris Droz, and Lenny H. E. Winkel\*



Cite This: *Environ. Sci. Technol.* 2021, 55, 5547–5558



Read Online

ACCESS |



Metrics & More



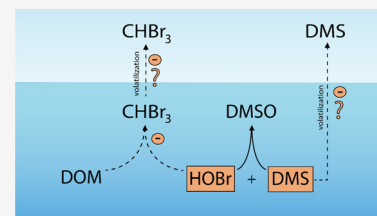
Article Recommendations



Supporting Information

**ABSTRACT:** Recently, we suggested that hypobromous acid (HOBr) is a sink for the marine volatile organic sulfur compound dimethyl sulfide (DMS). However, HOBr is also known to react with reactive moieties of dissolved organic matter (DOM) such as phenolic compounds to form bromoform (CHBr<sub>3</sub>) and other brominated compounds. The reaction between HOBr and DMS may thus compete with the reaction between HOBr and DOM. To study this potential competition, kinetic batch and diffusion-reactor experiments with DMS, HOBr, and DOM were performed. Based on the reaction kinetics, we modeled concentrations of DMS, HOBr, and CHBr<sub>3</sub> during typical algal bloom fluxes of DMS and HOBr ( $10^{-13}$  to  $10^{-9}$  M s<sup>-1</sup>). For an intermediate to high HOBr flux ( $\geq 10^{-11}$  M s<sup>-1</sup>) and a DMS flux  $\leq 10^{-11}$  M s<sup>-1</sup>, the model shows that the DMS degradation by HOBr was higher than for photochemical oxidation, biological consumption, and sea–air gas exchange combined. For HOBr fluxes  $\leq 10^{-11}$  M s<sup>-1</sup> and a DMS flux of  $10^{-11}$  M s<sup>-1</sup>, our model shows that CHBr<sub>3</sub> decreases by 86% compared to a lower DMS flux of  $10^{-12}$  M s<sup>-1</sup>. Therefore, the reaction between HOBr and DMS likely not only presents a sink for DMS but also may lead to suppressed CHBr<sub>3</sub> formation.

**KEYWORDS:** bromine, dissolved organic matter, kinetics, diffusion, degradation



## INTRODUCTION

In marine systems, hypobromous acid (HOBr) is an active form of bromine (Br), produced via the enzymatic reaction between bromide (Br<sup>-</sup>) and hydrogen peroxide (H<sub>2</sub>O<sub>2</sub>).<sup>1</sup> This reaction is catalyzed by vanadium-bromoperoxidase enzymes (V-BrPO), which are widely distributed in marine organisms, such as macroalgae,<sup>2–5</sup> microalgae,<sup>6–8</sup> and bacteria.<sup>9–12</sup> Once produced, HOBr reacts fast with phenolic compounds (PhOH) and other reactive moieties such as  $\alpha,\beta$ -diketones of dissolved organic matter (DOM), to form polybrominated compounds including volatile organic compounds (VOCs),<sup>1,8,13–16</sup> of which bromoform (CHBr<sub>3</sub>) is the most abundant chemical species.<sup>6,13,17–19</sup> Brominated VOCs are of environmental concern, because after their release into the atmosphere, they are photolytically decomposed to Br atoms (Br•),<sup>20,21</sup> which together with other reactive halogen species (RHS) play a key role in the chemistry and oxidizing capacity of the troposphere.<sup>22</sup> RHS depletes ozone (O<sub>3</sub>)<sup>23–25</sup> via efficient catalytic cycles in the troposphere and stratosphere, reduces the lifetime of the greenhouse gas methane (CH<sub>4</sub>),<sup>26</sup> and reacts with dimethyl sulfide (DMS) in the troposphere,<sup>27</sup> thereby affecting climatic processes.

Similar to HOBr, DMS, a volatile organic sulfur (S) compound, is biologically produced in seawater and it also plays a role in atmospheric chemistry and climate as it promotes the formation of aerosols and clouds through its oxidation to sulfate.<sup>28–31</sup> The main pathway of DMS production is via enzymatic cleavage of its precursor dimethylsulfoniopropionate (DMSP).<sup>32</sup> Whereas HOBr is

assumed to be generally extracellularly produced because V-BrPO (the most common form of haloperoxidase in the marine environment)<sup>33</sup> is often described to be located in the apoplast,<sup>1,8,13,34</sup> the production of DMS is less site-specific. While DMSP is synthesized intracellularly,<sup>32,35,36</sup> its cleavage to DMS may occur intra-<sup>37–40</sup> or extracellularly,<sup>41–44</sup> depending on the location of the DMSP-lyase enzyme. According to Stefels et al. (2007),<sup>32</sup> a facilitated removal of excess S and maintenance of an intracellular nitrogen (N) balance (overflow hypothesis) support the extracellular cleavage of DMSP to DMS,<sup>45</sup> whereas the DMSP-based antioxidative system described by Sunda et al. (2002)<sup>46</sup> would favor an intracellular (e.g., chloroplastic) location of the lyase enzymes. Antioxidative properties were reported for DMSP and DMS,<sup>46</sup> for example, several studies report an upregulation of DMSP and DMS under conditions of oxidative stress.<sup>46–50</sup> In parallel, increased bromination activity was also observed under oxidative stress conditions.<sup>51–53</sup> Amplified HOBr production is often associated with a reduction of H<sub>2</sub>O<sub>2</sub> levels and thus provides protection of the cell against oxidative damage, similar to DMS.<sup>54</sup> Production of DMS and HOBr may also be motivated by defense mechanisms, as for both HOBr<sup>55</sup> and

**Received:** December 3, 2020

**Revised:** March 16, 2021

**Accepted:** March 17, 2021

**Published:** March 31, 2021



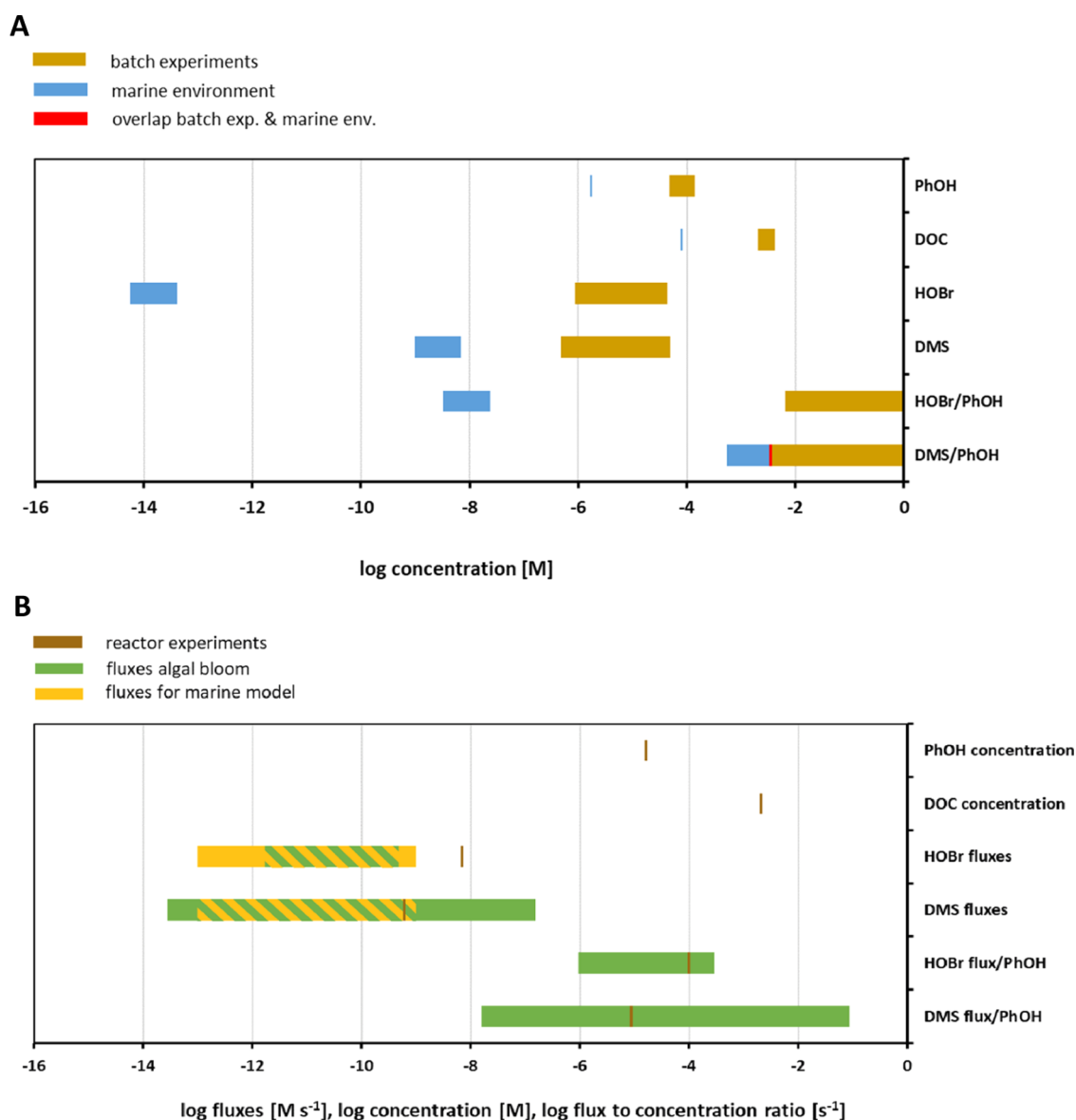


**Figure 1.** Comparison of natural, experimental, and modeled concentrations of HOBr, DMS, phenol, and flux ranges of HOBr and DMS. (A): DMS, HOBr, DOC, and phenol concentrations and the corresponding DMS/phenol and HOBr/phenol concentration ratios for batch experiments and the marine environment. (B): Natural DMS and HOBr flux ranges and flux ranges in diffusion-reactor experiments and marine model calculations, DOC and phenol concentrations of diffusion-reactor experiments, and DMS flux/phenol concentration and HOBr flux/phenol concentration ratios of diffusion-reactor experiments. Phenol and DOC concentrations have the unit “molar” (M), whereas fluxes have the unit molar per second ( $\text{M s}^{-1}$ ). Flux to phenol concentration ratios have the unit per second ( $\text{s}^{-1}$ ). Natural DMS concentration was taken from Lana et al. (2011);<sup>78</sup> natural HOBr concentration range was from Müller et al. (2019);<sup>62</sup> surface DOC concentration was from Benner et al. (1992);<sup>79</sup> and phenolic moiety concentrations were from this study (see Text S4, [Supporting Information](#)). Natural DMS and HOBr fluxes in algal blooms are discussed in Text S5, [Supporting Information](#). DMS and HOBr concentrations and the corresponding DMS and HOBr to phenolic moiety concentration ratios used in batch experiments are discussed in Text S7, [Supporting Information](#). DMS and HOBr fluxes used in diffusion-reactor experiments are discussed in Text S12, [Supporting Information](#).

DMSP lyase products,<sup>56,57</sup> antimicrobial properties were reported. It is likely that both HOBr and DMS are produced during the same algal bloom event, for example, high production rates of both DMS<sup>58,59</sup> and HOBr<sup>8,51/CHBr<sub>3</sub></sup><sup>60,61</sup> have been reported for ice algae in polar regions and the coincident production of DMS and HOBr was also documented for a marine diatom species.<sup>58,60</sup>

We recently demonstrated a high reactivity between HOBr and DMS,<sup>62</sup> with a second-order rate constant of  $2 \times 10^9 \text{ M}^{-1} \text{ s}^{-1}$ , which is three to four orders of magnitude higher than the reactivity of HOBr with phenol at pH 8.<sup>63</sup> Based on this

second-order rate constant and estimated marine HOBr concentrations,<sup>62</sup> we previously suggested that HOBr represents a globally important, but yet unidentified, sink for marine DMS, of similar quantitative importance as other known DMS sinks, that is, bacterial consumption, photochemical oxidation, and air–sea gas exchange. Furthermore, although DMS is present in lower concentrations in marine waters than phenolic moieties in DOM, due to its high reactivity, it might compete with the reaction between marine DOM and HOBr and consequently affect the formation of CHBr<sub>3</sub> and other brominated VOCs. However, the potential

competition between DMS and the more predominant DOM moieties for their reaction with HOBr in marine waters has not been studied yet. In this study, we investigated (i) the influence of DMS on the production of brominated VOCs by HOBr in the presence of DOM and (ii) the DMS oxidation by HOBr at DMS/DOM ratios relevant for the marine environment. Two types of DOM extracts with low aromatic fractions were used as surrogates for marine DOM. Kinetic studies were carried out using batch experiments for relevant concentration ratios of DMS/phenolic moieties and in custom-built diffusion reactors for relevant DMS flux/phenolic moiety ratios and HOBr flux/phenolic moiety ratios. Finally, the results of diffusion-reactor experiments were validated using a diffusion-reaction model, which was extended to cover a wide range of natural HOBr and DMS fluxes to study the reactions between HOBr, DMS, and DOM for various environmentally relevant scenarios.

## MATERIALS AND METHODS

**Production of Stock Solutions and Standards.** Stock solutions of dimethyl sulfide (DMS,  $(\text{CH}_3)_2\text{S}$ , 99%, Sigma-Aldrich, St. Louis, USA), hypobromous acid (HOBr), oxidized S compounds (i.e., dimethyl sulfoxide, DMSO  $(\text{CH}_3)_2\text{SO}$ ; dimethyl sulfone,  $\text{DMSO}_2$   $(\text{CH}_3\text{SO})_2$ ; methane sulfonic acid,  $\text{CH}_3\text{SO}_3\text{H}$ ; and sodium sulfate,  $\text{Na}_2\text{SO}_4$ ), and 2,2-azino-bis(3-ethylbenzothiazoline)-6-sulfonic acid-diammonium salt (ABTS,  $\text{C}_{18}\text{H}_{18}\text{N}_4\text{O}_6\text{S}_4$ , >98%, Sigma-Aldrich, St. Louis, USA) were produced as described in Müller et al. (2019)<sup>62</sup> (see also Table S1).

Stock solutions of 500 mg  $\text{L}^{-1}$  DOM in ultrapure water were produced from the International Humic Substances Society's (IHSS) "Upper Mississippi River NOM" (UMRNOM, cat no: 1R110N; IHSS, St. Paul, USA) and the "Pony lake fulvic acid" (PLFA, cat no: 1R109F; IHSS, St. Paul, USA) and stored in amber glass vials after the pH was set to ca. 10<sup>64</sup> with sodium hydroxide solution (NaOH, 32%, Merck, Darmstadt, Germany). The NOM stock solutions were then sonicated for 2 × 10 min in an ultrasonic bath (SONOREX Super 10 P, Berlin, Germany), followed by a readjustment of the pH value to the target pH,<sup>64</sup> using a diluted nitric acid solution (10%; 1.7 M) ( $\text{HNO}_3$ , Roth,  $\text{HNO}_3$  Suprapur 69%). The NOM stock solutions were stored at 4 °C and used within 1 week.

A VOC-mix standard (1000  $\mu\text{g mL}^{-1}$  each in methanol, composition given in Table S2) was obtained from Supelco (Bellefonte, USA) of which an aqueous stock solution of 0.1 mg  $\text{L}^{-1}$  was produced in a gas-tight amber glass vial a few hours before use. DMS was added to this solution at 10<sup>-5</sup> M concentration (Text S3, Supporting Information).

**Natural Organic Matter Standards Used and Their Phenolic Content.** Previous kinetic experiments with HOBr and NOM showed that PLFA is the best proxy for marine DOM with respect to brominated trihalomethane (THM) formation.<sup>65</sup> Furthermore, its carbon to nitrogen ratio (C/N) is  $\approx 8$ , which is similar to the C/N ratio of marine DOM.<sup>65</sup>

PLFA has a low aromatic fraction of 12% (which is the lowest of all aquatic and terrestrial OM reference standards from IHSS)<sup>66</sup> based on <sup>13</sup>C NMR Estimates of Carbon Distribution. However, PLFA has a very limited availability, only permitting a small number of experiments. UMRNOM was selected as a second reference standard for marine DOM, which also has a low aromatic fraction of 19% (based on <sup>13</sup>C NMR Estimates of Carbon Distribution).<sup>66</sup> The phenolic contents of PLFA and UMRNOM have been previously

determined via analysis of the electron-donating capacity, resulting in 1.77 mmol phenol  $\text{g}^{-1}$  C for PLFA<sup>65,67</sup> and 2.8 mmol phenol  $\text{g}^{-1}$  C for UMRNOM.<sup>68</sup> Batch experiments performed with 50 mg  $\text{L}^{-1}$  PLFA (26.2 mg C  $\text{L}^{-1}$ ) thus correspond to 46.5  $\mu\text{mol phenol L}^{-1}$ , whereas for UMRNOM concentrations of 50 and 100 mg  $\text{L}^{-1}$  (25 and 50 mg C  $\text{L}^{-1}$ ) correspond to 70 and 140  $\mu\text{mol phenol L}^{-1}$ , respectively.

An overview of the used concentration ranges of DMS, HOBr, DOM, and phenolic compounds in batch experiments and how these compare to naturally occurring concentration ranges is shown in Figure 1A. It should be noted that HOBr concentrations used in batch experiments are much higher than actual HOBr concentrations in marine waters. These high levels of HOBr were necessary to quantify the reactants and reaction products. However, as we used environmentally relevant DMS/DOM (phenolic compound) concentration ratios, a similar fraction of HOBr is expected to react with DMS in batch experiments as under natural conditions.

DMS and HOBr fluxes in diffusion-reactor experiments and used flux ranges in a diffusion-reaction model (presented later) in comparison to typical DMS and HOBr fluxes during algal-bloom conditions are shown in Figure 1B. The different concentration ranges, flux ranges, concentration to PhOH ratios, and flux to PhOH ratios shown in Figure 1 were determined based on (i) the natural PhOH, DMS, and HOBr concentration ranges (Text S4, Supporting Information), (ii) the natural DMS and HOBr fluxes occurring in algal blooms (Text S5, Supporting Information), and (iii) the experimental DMS, HOBr, and PhOH concentrations and DMS and HOBr fluxes (Tables S5–S7).

**Kinetic Experiments.** Kinetic experiments with HOBr, DMS, and DOM were carried out in a simplified seawater medium containing typical concentrations of  $\text{Cl}^-$  and  $\text{Br}^-$  (0.55 M sodium chloride, NaCl: Merck, >99.5% and 840  $\mu\text{M}$  potassium bromide, KBr: Sigma-Aldrich, >99%).<sup>69</sup> It was shown in a previous study that the contribution of other reactive Br species (i.e.,  $\text{Br}_2$ ,  $\text{BrCl}$ , and  $\text{Br}_2\text{O}$ ) to the oxidation of DMS is insignificant compared to that of HOBr.<sup>62</sup> Before use, NaCl was recrystallized with a rotary evaporator to reduce the concentration of impurities, especially iodide ( $\text{I}^-$ ), which could potentially react with HOBr to produce hypoiodous acid and eventually iodate.<sup>70</sup> The seawater medium was buffered with 50 mM phosphate ( $\text{NaH}_2\text{PO}_4$ , > 99–102%, Merck, Darmstadt, Germany and  $\text{Na}_2\text{HPO}_4$ , Sigma-Aldrich, St. Louis, USA). The pH of the solution was measured before and after each experiment and it did not deviate more than 0.05 units from the target pH.

**Batch Experiments.** Two series of batch experiments were performed. In the first series, variable DMS concentrations but constant HOBr and DOM concentrations were used to study the influence of DMS on the formation of THMs. In the second series, variable HOBr concentrations and constant DMS and DOM concentrations were used to investigate the role of HOBr in DMS consumption. Detailed information on these batch experiments, that is, concentrations of DMS, HOBr, concentrations of DOM/phenolic moieties, and concentration ratios of phenolic moieties to HOBr and DMS are provided in Table S5. Experiments in the absence of DOM were not conducted in this study as (i) the reactivity between HOBr and DMS in the absence of DOM was studied previously<sup>62</sup> and is characterized by a quick and quantitative oxidation of DMS and (ii) bromoform and other THMs are not produced in the absence of DOM.

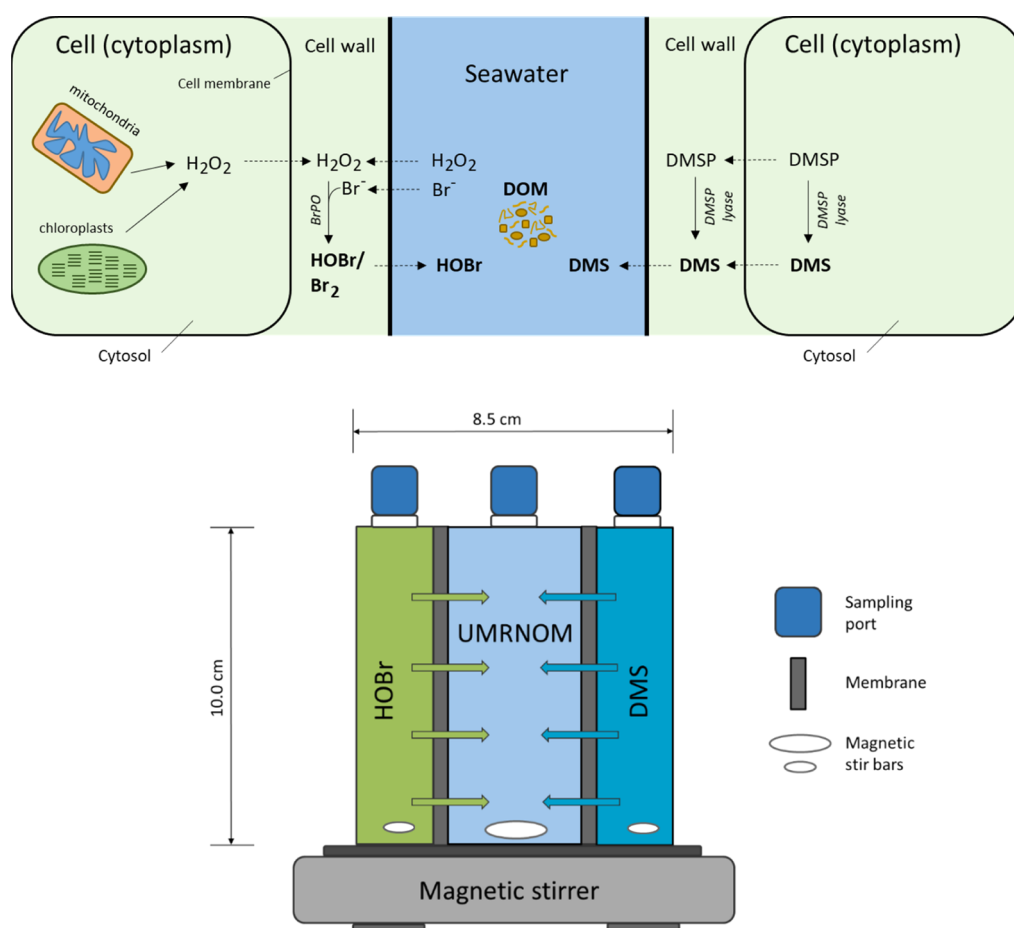


**Figure 2.** Simplified schematic representation of two algal cells separated by seawater (top) and the diffusion-reactors mimicking this situation (bottom). For simplicity, only the pathway of DMS production via DMSP lyase is indicated in the top figure. The reactor system is a simplified system, assuming that HOBr and DMS react in seawater. Potentially, HOBr and DMS may also react in the phycosphere,<sup>80</sup> however, this was not studied here. The two outer chambers (corresponding to algal cells) are separated from the middle chamber (corresponding to the surrounding seawater) by semipermeable nanofiltration membranes. The outer chambers are filled with simplified artificial seawater solutions containing HOBr and DMS, respectively, which diffuse to the middle chamber containing DOM (UMRNOM) in artificial seawater.

Experiments were carried out at pH 8 (present day ocean pH) and pH 7.5 (projected future ocean pH at high latitudes in 2100).<sup>71</sup> All glassware (i.e., 10 mL ND20 headspace amber crimp vials, 46 × 22.5 mm, BGB Analytics, Bockten, Switzerland) was cleaned in a 0.5% nitric acid bath (Roth, HNO<sub>3</sub> Suprapur 69%) for 24 h, rinsed with ultrapure water and methanol, and dried under the fume hood before use.

Reactions between HOBr, DOM, and DMS were carried out in 10 mL gastight headspace amber vials (final volume = 10 mL) (ND20 46 × 22.5 mm, with a magnetic crimp cap and a 8 mm hole with silicone/PTFE septa) under magnetic stirring. Buffer media, DOM and DMS, were added to the vials in advance and the reaction was initiated by injecting 5 mL of a HOBr solution (a 1:1 volumetric ratio). Details of the concentrations are given in Table S5 (see also Text S7, Supporting Information). For practical reasons, higher than natural HOBr/phenolic and DMS/phenolic moiety ratios were applied (Text S6, Supporting Information). For experiments with constant DMS concentrations (0.5 μM), there is a small overlap of the DMS/phenolic moiety ratio with the corresponding ratio for natural conditions (Figure 1A).

For all experiments, a reaction time of 10 min was used for practical reasons, that is, to enable sampling at manageable time intervals. Furthermore, this reaction time warrants

complete reactions between DMS, DOM, and HOBr ( $t_{1/2} < 0.01$  s). After a reaction time of 10 min, NaNO<sub>2</sub> was added (final concentration: 100 μM) to quench potentially residual HOBr. The quenched solution was subsequently transferred to 10 mL gastight headspace vials (1:10 dilution) and HPLC vials (EcoLine 1.5 mL crimp amber vials; BGB Analytics, Bockten, Switzerland).

**Diffusion-Reactor Experiments.** To mimic the natural marine DMS and HOBr diffusion fluxes in kinetic experiments, diffusion-reactors were constructed. A detailed overview of their design and used materials is provided in Text S8, Supporting Information. Briefly, the diffusion-reactors consist of two outer chambers (one for a DMS solution and one for a HOBr solution) and a middle chamber (UMRNOM solution) with volumes of 45, 48, and 56 mL, respectively (Figure 2). The outer chambers are separated from the middle chamber by nanofiltration membranes (HOBr diffusion: GE Osмотics, HL series, General Electric Power & Water; DMS diffusion: SIL-TEC sheeting, P/N 500-1, Technical Products Inc. of GA, Georgia, USA) (Texts S8 and S9, Supporting Information), which control the diffusion of HOBr and DMS, respectively, from the outer to the inner chamber. The membranes were selected on the basis of diffusion tests (Figures S2 and S3). Similar to batch experiments, competition kinetics in the inner

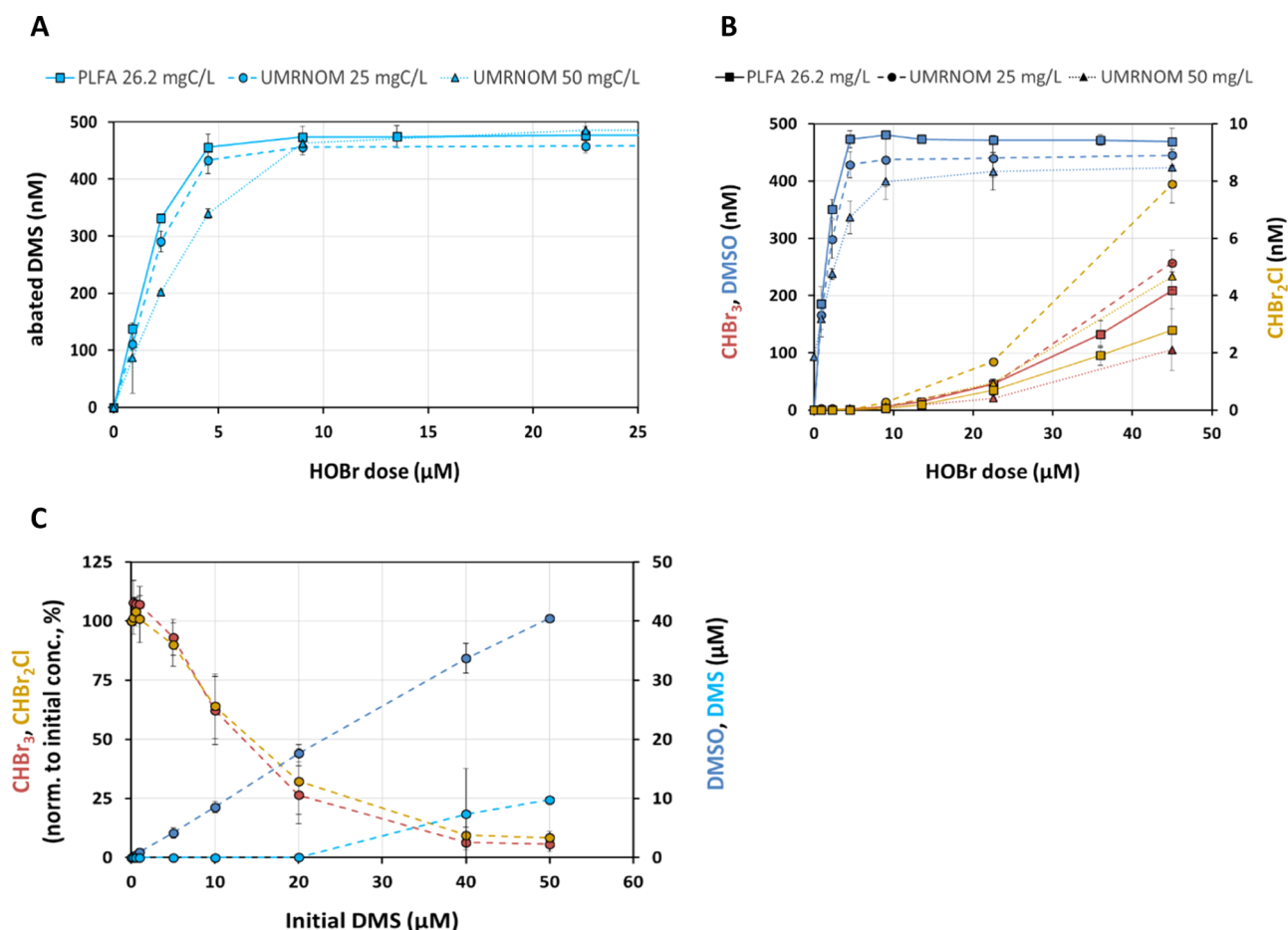


**Figure 3.** Batch experiments for the reactions between DMS, DOM, and HOBr in buffered artificial seawater at pH 8 ( $[\text{PO}_4]_{\text{tot}} = 25 \text{ mM}$ ,  $[\text{NaCl}] = 0.55 \text{ M}$ , and  $[\text{KBr}] = 840 \mu\text{M}$ ). The reaction time was always 10 min. Data without DOM have been provided previously (Müller et al. *ES&T*, 2019). (A) Abated DMS (initial concentrations 458 and 489 nM for duplicate experiments) as a function of variable HOBr doses (0–45  $\mu\text{M}$ ) in the presence of 26.2 mg C L<sup>-1</sup> PLFA (squares, solid line), 25 mg C L<sup>-1</sup> UMRNOM (circles, dashed line), or 50 mg C L<sup>-1</sup> UMRNOM (triangles, dotted line). Each data point represents duplicate experiments. (B) Measured DMSO, CHBr<sub>3</sub>, and CHBr<sub>2</sub>Cl concentrations for the same experiment as presented in (A). (C) Concentrations of DMS and DMSO and the relative concentrations of CHBr<sub>3</sub> and CHBr<sub>2</sub>Cl (normalized to the sample with DMS = 0  $\mu\text{M}$ ) after the reaction of 45  $\mu\text{M}$  HOBr with 25 mg C L<sup>-1</sup> UMRNOM and DMS at variable doses (0–50  $\mu\text{M}$ ). Data points represent four experimental replicates.

chamber were applied to study reactions of HOBr with both DMS and DOM.

After the diffusion-reactor parts were assembled (Text S10, Supporting Information), all chambers were filled with a buffered artificial seawater solution avoiding any headspace. Thereafter, all additions of solutions (DOM, DMS, and HOBr) and sampling steps were performed by gastight syringes, using sampling ports with septa. The duration of the diffusion-reaction experiments was limited to 2 h. The experimental procedure is described in detail in Text S11, Supporting Information. HOBr concentrations from the HOBr chamber at  $t = 0$  and  $t = 120 \text{ min}$  were photometrically quantified immediately after sampling using the ABTS-method.<sup>72</sup> For HOBr, initial tests had indicated HOBr loss in the HOBr chamber, which could not be explained by HOBr diffusion alone. Therefore, the HOBr fluxes were estimated based on the polynomial regression of the HOBr–CHBr<sub>3</sub> and HOBr–CHBr<sub>2</sub>Cl relationships from batch experiments (Figure S4). Although the fluxes in diffusion-reactor experiments are at the upper end of reported fluxes in algal blooms (DMS) or exceed them (HOBr), the HOBr flux to PhOH concentration ratios are relatively close to natural conditions owing to the higher

than natural PhOH concentrations (Text S12, Supporting Information).

To validate the experimental data and predict concentrations of DMS, DMSO, CHBr<sub>3</sub>, and CHBr<sub>2</sub>Cl (Text S12, Supporting Information) as a function of the experiment-specific HOBr and DMS diffusion fluxes, a chemical diffusion-reaction model was built with Kintecus software<sup>73</sup> (Table S8). With the determined HOBr and DMS diffusion rates (Text S12, Supporting Information), the kinetics of DMS–HOBr<sup>62</sup> and phenolic moieties–HOBr reactions,<sup>74</sup> model calculations were performed and compared to measured DMS and DMSO concentrations (Table S8). However, CHBr<sub>3</sub> and CHBr<sub>2</sub>Cl concentrations were not modeled because the formation of these compounds is complex, involving multiple reaction pathways. Bromination of UMRNOM is not well constrained in the scientific literature and attempting to model this process would introduce significant uncertainty.

**Modeling Concentrations of DMS, HOBr, and CHBr<sub>3</sub> for Natural DMS and HOBr Fluxes.** The batch and diffusion-reactor experiments in this study represent simplified DMS–DOM–HOBr systems. To study more realistic conditions, that is, accounting for natural marine DMS and

HOBr fluxes, and to test which fluxes lead to a substantial reduction in concentrations of DMS, HOBr, or  $\text{CHBr}_3$ , a diffusion-reaction model was developed. The influence of typical algal bloom DMS fluxes ( $10^{-13}$  to  $10^{-9}$   $\text{M s}^{-1}$ ) on HOBr and  $\text{CHBr}_3$  concentrations was calculated for a range of natural HOBr fluxes ( $10^{-13}$  to  $10^{-9}$   $\text{M s}^{-1}$ ) (Text S14, Supporting Information), and vice versa the influence of this range of HOBr fluxes on DMS concentrations was tested (Text S14, Supporting Information).

Besides DMS and HOBr fluxes, the model included the following processes and reactions:

(a) DMS reaction with HOBr and other oxidants [ $\text{O}_3$ , hypiodous acid (HOI), and  $\text{H}_2\text{O}_2$ ], (b) known DMS sinks [i.e., sea–air gas exchange ( $k_{\text{sea-air}}$ ), bacterial consumption ( $k_{\text{bact}}$ ), photochemical oxidation ( $k_{\text{photo}}$ )], (c) reactions of HOBr with phenolic moieties of DOM, considering the kinetics and efficiency of  $\text{CHBr}_3$  formation, (d) sea–air gas exchange of  $\text{CHBr}_3$  (as the major sink for marine  $\text{CHBr}_3$ ), (e) other reactions with HOBr, that is, with iodide and bromide ( $\text{Br}^-$ ), (f) iodine, bromine–, and mixed iodine–bromine reactions of reactive products from initial reactions (e.g., HOI), and (g) abiotic formation of HOBr and HOI (oxidation of  $\text{Br}^-$  and  $\text{I}^-$  by  $\text{O}_3$ ; oxidation of  $\text{I}^-$  by HOBr). Potential reduction of DMSO to DMS was not taken into account in this study. Further details on the model, including the rate constants and concentrations, are provided in Text S14.1, Supporting Information.

Although not experimentally studied, we also included the reaction of DMS with HOI in our model, with an estimated reactivity of  $10^4 \text{ M}^{-1} \text{ s}^{-1}$  (Text S14.2, Supporting Information). HOI and HOCl production from algae were not included in our model, for reasons explained in Text S14.3, Supporting Information.

The model was run for 24 h. Steady-state concentrations for compounds (i.e., phenol,  $\text{O}_3$ ,  $\text{H}_2\text{O}_2$ ,  $\text{I}^-$ ,  $\text{Br}^-$ ,  $\text{Cl}^-$ ,  $\text{H}^+$ , and  $\text{OH}^-$ ) were used, assuming that diffusion processes will balance out reaction-induced local species depletion by transport of these compounds from the surrounding water.

**Analyses of DMS, THMs, DMS Oxidation Products, and HOBr.** Concentrations of DMS and THMs were quantified immediately after the experiment using direct-immersion solid-phase microextraction (DI-SPME) coupled to capillary gas chromatography–mass spectrometry (GC/MS), according to the method of Vriens et al. (2015).<sup>75</sup> DMS oxidation products were quantified within 1 week (storage at 4 °C) by HPLC (1200 series, Agilent Technologies) coupled to an ICP–MS/MS instrument (ICP–MS 8900, Agilent Technologies) as described in Müller et al. (2019).<sup>62</sup> The limits of quantification (LOQs) for DMS,  $\text{CHBr}_3$ , and  $\text{CHBr}_2\text{Cl}$  were  $1.7 \pm 1.4$ ,  $0.6 \pm 0.5$ , and  $0.6 \pm 0.5$  nM, respectively. The LOQ for DMSO was  $46.2 \pm 23.7$  nM, as reported in our previous study.<sup>62</sup> HOBr was quantified spectrophotometrically using the ABTS method at 405 nm (molar absorption coefficient:  $31,600 \text{ M}^{-1} \text{ cm}^{-1}$ ), as described in Pinkernell et al. (2000).<sup>72</sup>

## RESULTS AND DISCUSSION

**Reactions of HOBr with DMS and DOM in Batch Experiments.** *Influence of DOM Type and Concentration on the Consumption of DMS and Formation of DMSO.* In the experiments using variable HOBr doses (DMS being held constant at around 500 nM, i.e., between  $458 \pm 11$  and  $489 \pm 2$ ), the DMS consumption increased steeply with increasing

HOBr for all DOM types and concentrations (Figure 3A). For HOBr doses  $< 9 \mu\text{M}$ , the highest proportion of abated DMS was observed for samples containing  $26.2 \text{ mg C L}^{-1}$  PLFA. Similar DMS concentrations were abated for samples containing  $25 \text{ mg L}^{-1}$  UMRNOM, whereas significantly less DMS was abated in samples with  $50 \text{ mg C L}^{-1}$  UMRNOM. For HOBr doses  $\geq 9 \mu\text{M}$ , DMS was below the LOQ ( $< 1.7$  nM) for all DOM types and concentrations. A complete consumption of DMS by HOBr is remarkable considering the large excess of highly reactive phenolic moieties relative to DMS (molar phenolic moiety/DMS ratio for  $26.2 \text{ mg C L}^{-1}$  PLFA: 94; for  $25 \text{ mg C L}^{-1}$  UMRNOM: 140; and for  $50 \text{ mg C L}^{-1}$  UMRNOM: 280). This can be explained by a higher apparent first order rate constant for the DMS–HOBr reaction, that is,  $k(\text{HOBr, DMS}) = 600 \text{ s}^{-1}$  than those for the phenol–HOBr reaction, that is,  $k(\text{HOBr, phenol}) = 41, 62$ , and  $124 \text{ s}^{-1}$  for  $26.2 \text{ mg C L}^{-1}$  PLFA,  $25 \text{ mg C L}^{-1}$  UMRNOM, and  $50 \text{ mg C L}^{-1}$  UMRNOM, respectively at pH 8 (all first-order rate constants were obtained from batch experiments in this study) (see also Text S6, Supporting Information). Therefore, it can be expected that the DMS–HOBr reaction outcompetes the reaction between HOBr and DOM moieties after the fastest reacting moieties (e.g., resorcinol) have been titrated away for higher HOBr doses.

DMSO was found to be the only product from the reaction between DMS and HOBr (Figure 3A). Also, in a previous study carried out in synthetic DOM-free seawater, we could demonstrate that DMSO is the final product of the stoichiometric reaction between HOBr and DMS.<sup>62</sup>

*Influence of DOM Type and Concentration on the Formation of THMs.* We identified  $\text{CHBr}_3$  and  $\text{CHBr}_2\text{Cl}$  as sole products of the reaction between DOM and HOBr in the batch experiments. None of the other 18 compounds present in the VOC mix (Table S2) were detected. With increasing HOBr doses,  $\text{CHBr}_3$  and  $\text{CHBr}_2\text{Cl}$  were produced nonlinearly with a stronger increase at higher HOBr doses. Furthermore,  $\text{CHBr}_3$  and  $\text{CHBr}_2\text{Cl}$  were only detected after DMS was completely exhausted (Figure 3B). Interestingly, the experiment with  $50 \text{ mg C L}^{-1}$  UMRNOM resulted in lower production of  $\text{CHBr}_3$  compared to  $25 \text{ mg C L}^{-1}$  (Figure 3B), which can be explained by the fact that in the presence of more HOBr-reactive sites, the multiple bromination steps required to produce  $\text{CHBr}_3$  are less likely.<sup>65</sup> In contrast, experiments conducted with  $26.2 \text{ mg C L}^{-1}$  PLFA resulted in a lower production of  $\text{CHBr}_3$  compared to  $25 \text{ mg C L}^{-1}$  UMRNOM (Figure 3B), likely due to about 40% lower content of phenolic moieties in PLFA compared to UMRNOM.<sup>65</sup> These results confirm that  $\text{CHBr}_3$  formation is favored by a high molar HOBr/DOC (or HOBr/phenolic moieties) concentration ratio and the absolute concentrations of phenolic moieties.<sup>65</sup>

For  $\text{CHBr}_2\text{Cl}$  production, we observed an even larger DOM-specific influence than for  $\text{CHBr}_3$ , with the highest production for experiments with  $25 \text{ mg C L}^{-1}$  UMRNOM, followed by  $50 \text{ mg C L}^{-1}$  UMRNOM and  $26.2 \text{ mg C L}^{-1}$  PLFA (Figure 3B). The  $\text{CHBr}_3/\text{CHBr}_2\text{Cl}$  concentration ratios were significantly higher in the presence of  $26.2 \text{ mg C L}^{-1}$  PLFA ( $77 \pm 23$ ; Welch-test,  $t_0 > t_v$ ; 0.975) compared to  $25 \text{ mg C L}^{-1}$  UMRNOM ( $24 \pm 18$ ). The  $\text{CHBr}_3/\text{CHBr}_2\text{Cl}$  concentration ratio for the PLFA experiment agrees well with observed  $\text{CHBr}_3/\text{CHBr}_2\text{Cl}$  ratios in the natural marine environment ( $\approx 65$ )<sup>76</sup> demonstrating again that PLFA is a good surrogate for natural marine DOM. We hypothesize that the chlorine in  $\text{CHBr}_2\text{Cl}$  originates from DOM and not from the artificial

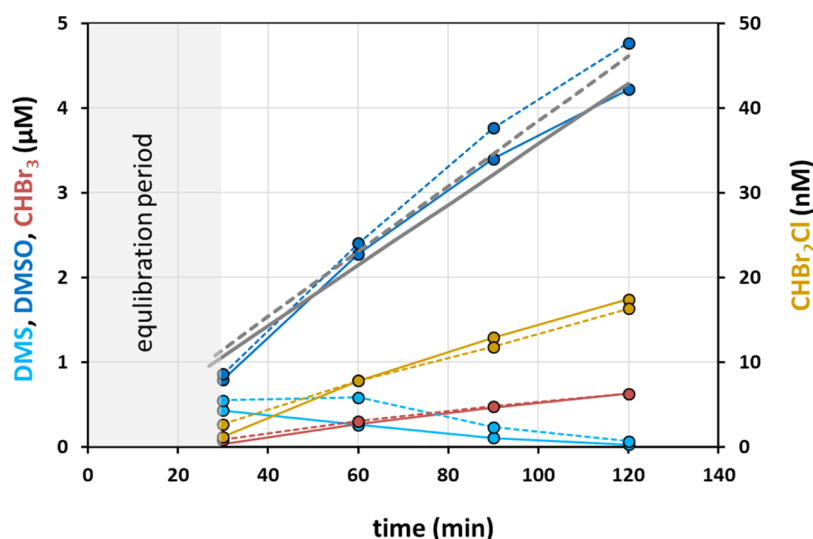


**Figure 4.** Time-course concentrations of DMS (light blue), DMSO (dark blue, modeled concentrations shown as gray lines), CHBr<sub>3</sub> (red), and CHBr<sub>2</sub>Cl (yellow) in the middle chamber for two diffusion-reactor experiments [R1 (solid lines) and R2 (dashed lines)]. Experimental conditions: pH 8, phosphate-buffered artificial seawater medium ([PO<sub>4</sub>]<sub>tot</sub> = 50 mM, [NaCl] = 0.55 M, and [KBr] = 840 μM) with an UMRNOM concentration of 25 mg C L<sup>-1</sup>. DMS and HOBr fluxes were quantified as  $6.0 \times 10^{-10}$  and  $9.8 \times 10^{-9}$  M s<sup>-1</sup> for R1 and  $6.4 \times 10^{-10}$  and  $1.0 \times 10^{-8}$  M s<sup>-1</sup> for R2, respectively (for details, see Text S12, Supporting Information). The middle chamber was sampled after 30, 60, 90, and 120 min. The gray band ( $t = 0-30$  min) represents the equilibration period for the system.

seawater matrix because experiments in the absence and presence of chloride yielded the same CHBr<sub>2</sub>Cl concentrations (Text S16, Supporting Information).

**Influence of Variable DMS Concentrations on the Formation of Br-THMs.** Figure 3C (pH 8) and Figure S5 (pH 7.5) show the evolution of Br-THMs, DMS, and DMSO for a constant HOBr concentration (45 μM) as a function of variable DMS doses in UMRNOM-containing buffered synthetic seawater. For DMS doses  $\leq 20$  μM, DMS was completely abated for HOBr doses of 45 μM in the presence of 25 mg C L<sup>-1</sup> UMRNOM for both pH 7.5 and 8 (Figures 3C and S5). For experiments with the highest DMS doses (40 and 50 μM), 10–20% of the initial DMS remains after the reaction. For these DMS doses, the HOBr dose (45 μM) is slightly over or understoichiometric, respectively. Because a fraction of HOBr is consumed by fast-reacting DOM moieties, not all DMS was oxidized to DMSO under these conditions, however, still the efficient oxidation of DMS indicates that HOBr is mainly consumed by DMS and not by DOM. Furthermore, the higher DMS concentrations resulted in an effective suppression of CHBr<sub>3</sub> and CHBr<sub>2</sub>Cl formation. For a dose of 50 μM DMS, the production of CHBr<sub>3</sub> and CHBr<sub>2</sub>Cl was suppressed to 5.7 and 8.4% of the blank value (corresponding to 0 μM DMS), respectively, at pH 8 (Figure 3C) and to 3.6 and 4.0%, respectively, at pH 7.5 (Figure S5). Overall, the results for DMS consumption/DMSO production and relative CHBr<sub>3</sub> and CHBr<sub>2</sub>Cl suppression are comparable for pH 8 (Figure 3C) and 7.5 (Figure S5). At both pH values, bromine is mainly present in its protonated form (HOBr fractions 0.86 and 0.95, for pH 8 and 7.5, respectively), which means that the bromine reactivity remains fairly constant. However, we observed on average a 37% higher CHBr<sub>3</sub> and 29% higher CHBr<sub>2</sub>Cl production at pH 8 than at pH 7.5 after a 10 min reaction time (Table S12). This can be explained by the maximum rate for the reaction between HOBr and phenol/phenolate being at pH 9.4 (pH for  $k_{\max} = 1/2(pK_1 + pK_2) = 1/2(8.8 + 10.0)$ ), which is closer to pH 8. Nevertheless, we do not expect a significant reduction in THM formation as a result of a potential pH

decrease from 8 to 7.5 because the reaction times in marine systems are much longer. However, ocean acidification may lead to changes in the marine community structure, HOBr production, and qualitative/quantitative changes in DOM among other factors, which may also affect THM production and these factors have not been investigated in this study.

To conclude, the performed batch experiments clearly showed that also in the presence of DOM (at relevant concentration ratios of DMS, HOBr, and organic moieties), DMS is efficiently consumed by HOBr. Formation of CHBr<sub>3</sub> and CHBr<sub>2</sub>Cl only occurred after DMS was depleted.

**Diffusion-Reactor Experiments.** Diffusion-reactor experiments were performed to mimic the dynamics of HOBr and DMS production and competition with DOM in a system including diffusion of DMS and HOBr. Before sampling, the system was allowed to equilibrate for 30 min to stabilize the HOBr flux into the middle chamber. Meanwhile, DMS started to decrease in the middle chamber (Figure 4). After 120 min, the concentration of DMS in the middle chamber was below (reactor 1; R1) or slightly above the LOQ (4.5 nM for reactor 2; R2), consistent with modeled DMS (Table S11). In contrast, concentrations of DMSO, CHBr<sub>3</sub>, and CHBr<sub>2</sub>Cl increased over time (Figure 4), as a result of the reactions of HOBr with DOM and DMS. The relatively low DMS concentrations in the middle chamber, in comparison to higher DMSO concentrations is explained by the high HOBr diffusion rate (with  $\Delta\text{HOBr}_{\text{diff}} > \Delta\text{DMS}_{\text{diff}}$ ) and the high DMS–HOBr reactivity, which lead to an almost complete oxidation of DMS to DMSO with an accumulation of DMSO.

The kinetic model (Table S8) indeed predicts DMS concentrations in the low nanomolar range after 120 min (Table S11) and successfully models the evolution of DMSO concentrations (gray lines in Figure 4; Table S11). DMSO is produced from progressive oxidation of DMS by HOBr. The steady increase of CHBr<sub>3</sub> and CHBr<sub>2</sub>Cl with increasing reaction time is explained by the reaction of diffused HOBr with DOM, implying that despite a rapid consumption of HOBr by DMS, sufficient HOBr is available to react with

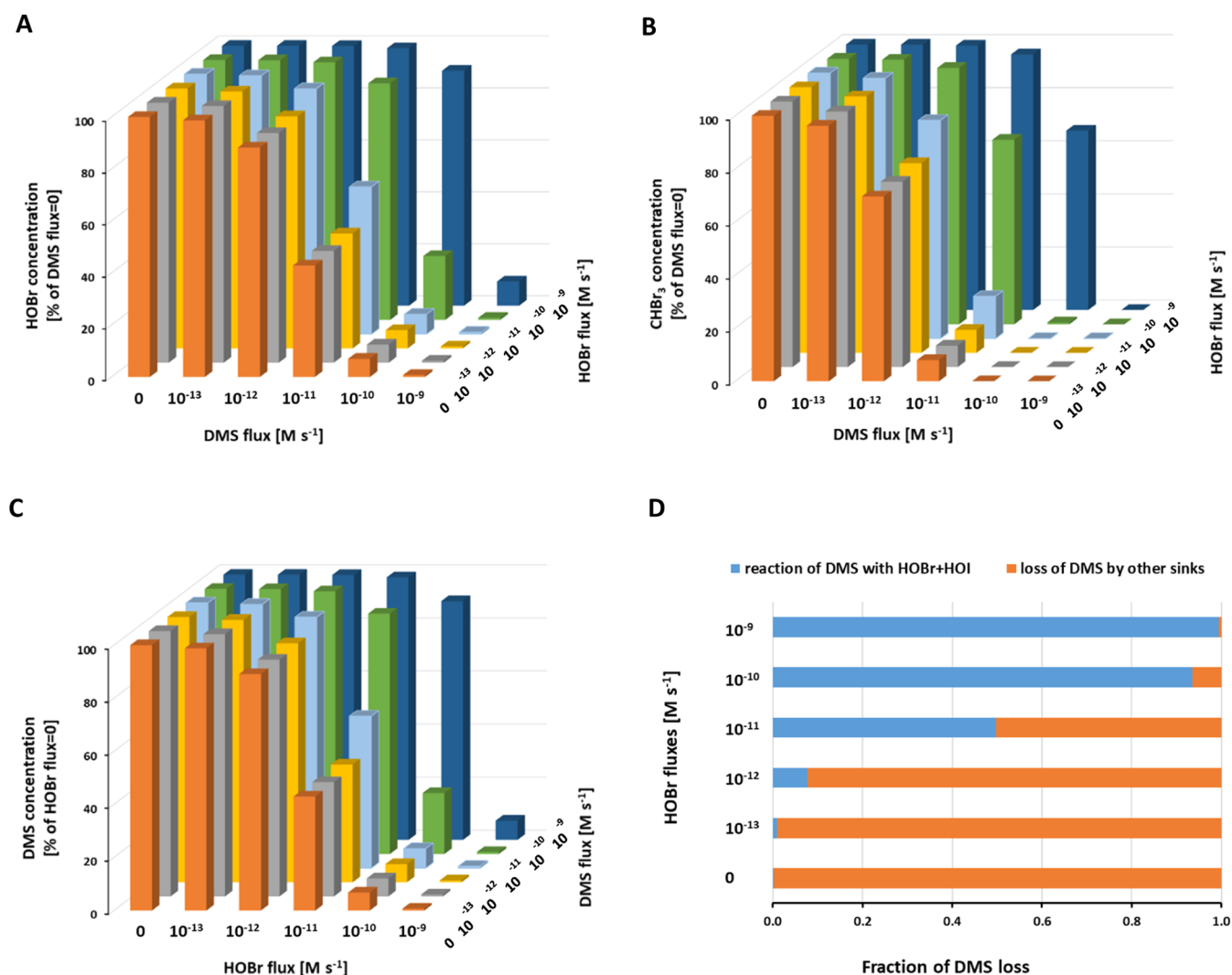


**Figure 5.** Modeled relative concentrations of HOBr, CHBr<sub>3</sub>, and DMS for typical HOBr and DMS fluxes (from the algal cells to the surrounding seawater) in the marine environment. The model run time was always 24 h. Absolute concentrations are provided in Table S13. (A): Influence of varying DMS and HOBr fluxes ( $0-1 \times 10^{-9} \text{ M s}^{-1}$ ) on relative HOBr concentrations that is indicated relative to a DMS flux of 0. (B): Influence of varying DMS and HOBr fluxes ( $0-1 \times 10^{-9} \text{ M s}^{-1}$ ) on relative CHBr<sub>3</sub> concentrations that is indicated relative to a DMS flux of 0. (C): Influence of varying DMS and HOBr fluxes ( $0-1 \times 10^{-9} \text{ M s}^{-1}$ ) on relative DMS concentrations that is indicated relative to a HOBr flux of 0. (D): Fraction of DMS reacting with HOBr and HOI in comparison to the main reported DMS sinks (DMS sea–air gas exchange, bacterial consumption, and photochemical oxidation), as a function of varying HOBr fluxes (0 to  $1 \times 10^{-9} \text{ M s}^{-1}$ ). The DMS flux was defined as  $1 \times 10^{-11} \text{ M s}^{-1}$ , representing an intermediate natural DMS flux. In all model calculations, a second-order rate constant of  $10^4 \text{ M}^{-1} \text{ s}^{-1}$  was assumed for the DMS–HOI reaction (see the discussion in Text S10, Supporting Information).

UMRNOM. For the same HOBr and DMS fluxes, the calculated fractions of HOBr reacting with DMS and phenolic moieties (i.e., phenol and brominated phenols) are 0.86 and 0.14, respectively.

Overall, the results of the diffusion-reactor experiments are in line with the findings of the batch experiments, indicating an efficient consumption of DMS by HOBr in the presence of DOM. Furthermore, these experiments showed that during the experiment, DMS concentrations decreased over time, while concentrations of DMSO, CHBr<sub>3</sub>, and CHBr<sub>2</sub>Cl increased, as a result of the reactions of HOBr with DMS and DOM, respectively.

**Model Calculations for Diffusion-Reactor Experiments Using Constant Phenol Concentrations.** The model based on the results of the diffusion-reactor experiments indicates that high HOBr fluxes result in a decrease of the concentrations of phenolic moieties from initially 70 to 26  $\mu\text{M}$  after 120 min

(Figure S6). However, in the marine environment, we expect fairly constant concentrations of phenolic moieties owing to their continuous production and diffusion processes. Therefore, the system was also modeled with a constant concentration of phenolic moieties (70  $\mu\text{M}$ ) to study the effect on DMSO concentrations. The results (Texts S16 and S17, Supporting Information) show that DMSO concentrations remain the same, whether or not the concentrations of phenolic moieties are varied. However, after 120 min the model indicates slightly higher DMS concentrations for constant concentrations of phenolic moieties (Figure S7), that is, 5.4 nM, than for variable concentrations of phenolic moieties (Figure S6), that is, 2.8 nM DMS. These slightly higher DMS concentrations are explained by a higher share of phenol reacting with HOBr than DMS reacting with HOBr, when concentrations of phenolic moieties remain constant.



**Model Simulations for the Marine Environment and the Implications.** To investigate the DMS–HOBr–DOM system more broadly, we modeled concentrations of DMS, HOBr, and  $\text{CHBr}_3$  as a function of a wide range of DMS and HOBr fluxes typical for algal blooms ( $10^{-13}$  to  $10^{-9}$   $\text{M s}^{-1}$ ) (Tables S3 and S4). The HOBr and DMS fluxes represent fluxes from the algal cells to the surrounding seawater. Tables S9 and S10 provide the details of the model and Figures S8 and S9 give the absolute concentrations of modeled HOBr,  $\text{CHBr}_3$ , and DMS concentrations as a function of the DMS and HOBr fluxes. Figure 5A shows concentrations of HOBr for the range of HOBr and DMS fluxes typical for algal blooms ( $10^{-13}$  to  $10^{-9}$   $\text{M s}^{-1}$ ) relative to the HOBr concentration in the absence of a DMS flux. Figure 5B shows concentrations of  $\text{CHBr}_3$  for the range of typical HOBr and DMS fluxes during algal blooms ( $10^{-13}$  to  $10^{-9}$   $\text{M s}^{-1}$ ) relative to the  $\text{CHBr}_3$  concentration in the absence of a DMS flux. Figure 5A,B shows that the reduction of HOBr and  $\text{CHBr}_3$  concentrations is the strongest for high DMS and low HOBr fluxes. In contrast, for HOBr fluxes equal or lower than  $10^{-11}$   $\text{M s}^{-1}$ , an increase in DMS flux from  $10^{-12}$  to  $10^{-11}$   $\text{M s}^{-1}$  leads to an average decrease in HOBr and  $\text{CHBr}_3$  concentrations by 48 and 86%, respectively. For HOBr fluxes at the upper end of estimated natural fluxes, that is, between  $10^{-10}$  and  $10^{-9}$   $\text{M s}^{-1}$ , an equal DMS flux is required to cause a substantial reduction in concentrations of HOBr and  $\text{CHBr}_3$  (Figure 5A,B). Figure 5C shows concentrations of DMS for the range of HOBr and DMS fluxes typical for algal blooms ( $10^{-13}$  to  $10^{-9}$   $\text{M}^{-1} \text{s}^{-1}$ ) relative to the DMS concentration in the absence of a HOBr flux. In analogy to the influence of HOBr and DMS fluxes on HOBr concentrations, an intermediate or higher HOBr flux ( $\geq 10^{-11}$   $\text{M s}^{-1}$ ) in combination with an intermediate or lower DMS flux ( $\leq 10^{-11}$   $\text{M s}^{-1}$ ) leads to a substantial reduction in DMS concentrations.

Although the extent of DMS consumption by HOBr clearly depends on the HOBr flux itself, also HOI, produced from the reaction between HOBr and  $\text{I}^-$ ,<sup>77</sup> could be a sink for DMS. Therefore, we compared DMS consumption by HOBr and HOI, both as a function of HOBr fluxes and different HOI–DMS reaction scenarios (Figure S10). Figure 5D illustrates the fraction of DMS consumed via reactions with HOBr and HOI and loss by known DMS sinks (photochemical degradation, bacterial consumption, and sea–air gas exchange) for varying HOBr fluxes. A higher fraction of DMS is consumed by HOBr in comparison to HOI for HOBr fluxes equal or higher than  $1 \times 10^{-12}$   $\text{M s}^{-1}$  (Figure S10). For HOBr fluxes lower than  $1 \times 10^{-11}$   $\text{M s}^{-1}$ , DMS loss is mainly controlled by other DMS sinks, that is, sea–air gas exchange, bacterial consumption, and photochemical oxidation.

Overall, our study confirms that HOBr can act as a sink for marine DMS. DMS can also act as a sink for HOBr, which may lead to a (partial) suppression of the formation of  $\text{CHBr}_3$  for a wide range of natural DMS and HOBr fluxes. Previous studies assumed that HOBr mainly reacts with DOM-moieties to produce brominated products.<sup>1,8</sup> However, they did not take into account the reaction of HOBr with DMS. Therefore, HOBr may affect the marine concentrations of DMS and  $\text{CHBr}_3$ , which could have implications for atmospheric DMS and  $\text{CHBr}_3$  concentrations via a reduced sea–air gas exchange of these compounds.

## ■ ASSOCIATED CONTENT

### Supporting Information

The Supporting Information is available free of charge at <https://pubs.acs.org/doi/10.1021/acs.est.0c08189>.

Procedure for the production of stock solutions of HOBr, DMS, oxidized S-species, and ABTS; list of the 18 compounds of the VOC-mix standard; production of stock solutions and standards; natural phenol, DMS, and HOBr concentrations and calculated DMS/phenol and HOBr/phenol ratios in seawater; estimations of the ranges of DMS and HOBr fluxes in algal blooms; specifications for the two types of batch experiments; batch experiments/experimental versus natural HOBr/phenolic moiety and DMS/phenolic moiety concentration ratios; construction of reactors and materials used; selection of membranes and determination of their diffusion rates for diffusion-reactor experiments; cleaning of reactor parts and membrane preparation; detailed procedure of diffusion-reactor experiments; calculations of DMS- and HOBr-fluxes for the diffusion-reactor experiments; diffusion-reaction model for reactor experiments; model for calculations of the influence of DMS- and HOBr-fluxes in the marine environment and assessment of the DMS–HOI reactivity; measured and modeled DMS and DMSO concentrations for diffusion-reactor experiments; hypothesis for the production of  $\text{CHBr}_2\text{Cl}$ ; reactions between HOBr and DMS in the presence of DOM in batch experiments at pH 7.5: variation of the initial DMS concentrations; kinetic simulations of the system HOBr–DMS–DOM in reactor experiment R1 (UMRNOM); kinetic modeling with constant phenol concentration; and modeled molar concentrations of HOBr,  $\text{CHBr}_3$ , and DMS for varying DMS and HOBr fluxes in the marine environment (PDF)

## ■ AUTHOR INFORMATION

### Corresponding Author

Lenny H. E. Winkel – Department of Water Resources and Drinking Water (W+T), Eawag, Swiss Federal Institute of Aquatic Science and Technology, CH-8600 Dübendorf, Switzerland; Department of Environment Systems (D-USYS), ETH Zurich, Swiss Federal Institute of Technology, Institute of Biogeochemistry and Pollutant Dynamics (IBP), 8092 Zürich, Switzerland; [orcid.org/0000-0001-7586-7256](https://orcid.org/0000-0001-7586-7256); Phone: +41 58 765 5601; Email: [lenny.winkel@eawag.ch](mailto:lenny.winkel@eawag.ch)

### Authors

Emanuel Müller – Department of Water Resources and Drinking Water (W+T), Eawag, Swiss Federal Institute of Aquatic Science and Technology, CH-8600 Dübendorf, Switzerland; Department of Environment Systems (D-USYS), ETH Zurich, Swiss Federal Institute of Technology, Institute of Biogeochemistry and Pollutant Dynamics (IBP), 8092 Zürich, Switzerland; [orcid.org/0000-0001-7683-2813](https://orcid.org/0000-0001-7683-2813)

Urs von Gunten – Department of Water Resources and Drinking Water (W+T), Eawag, Swiss Federal Institute of Aquatic Science and Technology, CH-8600 Dübendorf, Switzerland; Department of Environment Systems (D-USYS), ETH Zurich, Swiss Federal Institute of Technology,

Institute of Biogeochemistry and Pollutant Dynamics (IBP), 8092 Zürich, Switzerland; School of Architecture, Civil and Environmental Engineering (ENAC), École Polytechnique Fédérale de Lausanne (EPFL), 1015 Lausanne, Switzerland; [orcid.org/0000-0001-6852-8977](https://orcid.org/0000-0001-6852-8977)

**Sylvain Bouchet** – Department of Water Resources and Drinking Water (W+T), Eawag, Swiss Federal Institute of Aquatic Science and Technology, CH-8600 Dübendorf, Switzerland; Department of Environment Systems (D-USYS), ETH Zurich, Swiss Federal Institute of Technology, Institute of Biogeochemistry and Pollutant Dynamics (IBP), 8092 Zürich, Switzerland; [orcid.org/0000-0002-5753-9643](https://orcid.org/0000-0002-5753-9643)

**Boris Droz** – Department of Water Resources and Drinking Water (W+T), Eawag, Swiss Federal Institute of Aquatic Science and Technology, CH-8600 Dübendorf, Switzerland; Department of Environment Systems (D-USYS), ETH Zurich, Swiss Federal Institute of Technology, Institute of Biogeochemistry and Pollutant Dynamics (IBP), 8092 Zürich, Switzerland; [orcid.org/0000-0002-3942-704X](https://orcid.org/0000-0002-3942-704X)

Complete contact information is available at:  
<https://pubs.acs.org/10.1021/acs.est.0c08189>

## Notes

The authors declare no competing financial interest.

## ACKNOWLEDGMENTS

We thank Kristopher McNeill and Rachele Ossola for providing PLFA, Elisabeth Eiche for providing the VOC-mix standard, Jakov Bolotin for assistance with the GC/MS instrument, and Caroline Stengel for general support in the laboratory. Elia Ceppi is also acknowledged for carrying out initial batch experiments. Furthermore, we thank Jacqueline Traber for providing GE membranes for initial tests and Kay Fries for helping with the construction of PTFE reactors. This work was funded by Eawag and ETH Zurich (internal funds).

## REFERENCES

- Wever, R.; van der Horst, M. A. The role of vanadium haloperoxidases in the formation of volatile brominated compounds and their impact on the environment. *Dalton Trans.* **2013**, *42*, 11778–11786.
- Wever, R.; Tromp, M.; Van Schijndel, J.; Vollenbroek, E.; Olsen, R.; Fogelqvist, E. Bromoperoxidases: their role in the formation of HOBr and bromoform by seaweeds. *Biogeochemistry of Global Change*; Springer, 1993; pp 811–824.
- Hara, I.; Sakurai, T. Isolation and characterization of vanadium bromoperoxidase from a marine macroalga, *Ecklonia stolonifera*. *J. Inorg. Biochem.* **1998**, *72*, 23–28.
- Mehrtens, G. Haloperoxidase activities in Arctic macroalgae. *Polar Biol.* **1994**, *14*, 351–354.
- Rehder, D. Vanadate-dependent peroxidases in macroalgae: Function, applications, and environmental impact. *Oceanogr. Open Access* **2014**, *2*, 121.
- Moore, R. M.; Webb, M.; Tokarczyk, R.; Wever, R. Bromoperoxidase and iodoperoxidase enzymes and production of halogenated methanes in marine diatom cultures. *J. Geophys. Res. Oceans* **1996**, *101*, 20899–20908.
- Hughes, C.; Malin, G.; Nightingale, P. D.; Liss, P. S. The effect of light stress on the release of volatile iodocarbons by three species of marine microalgae. *Limnol. Oceanogr.* **2006**, *51*, 2849–2854.
- Hill, V. L.; Manley, S. L. Release of reactive bromine and iodine from diatoms and its possible role in halogen transfer in polar and tropical oceans. *Limnol. Oceanogr.* **2009**, *54*, 812–822.
- Van Pée, K.-H. Bacterial haloperoxidases and their role in secondary metabolism. *Biotechnol. Adv.* **1990**, *8*, 185–205.
- van Pée, K. H.; Lingens, F. Purification of bromoperoxidase from *Pseudomonas aureofaciens*. *J. Bacteriol.* **1985**, *161*, 1171–1175.
- Johnson, T. L.; Brahamsha, B.; Palenik, B.; Mühle, J. Halomethane production by vanadium-dependent bromoperoxidase in marine *Synechococcus*. *Limnol. Oceanogr.* **2015**, *60*, 1823–1835.
- Johnson, T. L.; Palenik, B.; Brahamsha, B. Characterization of a Functional Vanadium-dependent Bromoperoxidase in the Marine Cyanobacterium *Synechococcus* Sp. Cc93111. *J. Phycol.* **2011**, *47*, 792–801.
- Lin, C. Y.; Manley, S. L. Bromoform production from seawater treated with bromoperoxidase. *Limnol. Oceanogr.* **2012**, *57*, 1857–1866.
- Westerhoff, P.; Chao, P.; Mash, H. Reactivity of natural organic matter with aqueous chlorine and bromine. *Water Res.* **2004**, *38*, 1502–1513.
- Wever, R.; Tromp, M. G. M.; Krenn, B. E.; Marjani, A.; Van Tol, M. Brominating activity of the seaweed *Ascophyllum nodosum*: impact on the biosphere. *Environ. Sci. Technol.* **1991**, *25*, 446–449.
- Heeb, M. B.; Criquet, J.; Zimmermann-Steffens, S. G.; von Gunten, U. Oxidative treatment of bromide-containing waters: formation of bromine and its reactions with inorganic and organic compounds—a critical review. *Water Res.* **2014**, *48*, 15–42.
- Carpenter, L. J.; Liss, P. S. On temperate sources of bromoform and other reactive organic bromine gases. *J. Geophys. Res. Atmos.* **2000**, *105*, 20539–20547.
- Manley, S. L.; Goodwin, K.; North, W. J. Laboratory production of bromoform, methylene bromide, and methyl iodide by macroalgae and distribution in nearshore southern California waters. *Limnol. Oceanogr.* **1992**, *37*, 1652–1659.
- Laternus, F. Volatile halocarbons released from Arctic macroalgae. *Mar. Chem.* **1996**, *55*, 359–366.
- Barrie, L. A.; Bottenheim, J. W.; Schnell, R. C.; Crutzen, P. J.; Rasmussen, R. A. Ozone destruction and photochemical reactions at polar sunrise in the lower Arctic atmosphere. *Nature* **1988**, *334*, 138.
- McGivern, W. S.; Kim, H.; Francisco, J. S.; North, S. W. Investigation of the atmospheric oxidation pathways of bromoform and dibromomethane: Initiation via UV photolysis and hydrogen abstraction. *J. Phys. Chem. A* **2004**, *108*, 7247–7252.
- Saiz-Lopez, A.; von Glasow, R. Reactive halogen chemistry in the troposphere. *Chem. Soc. Rev.* **2012**, *41*, 6448–6472.
- Daniel, J. S.; Solomon, S.; Portmann, R. W.; Garcia, R. R. Stratospheric ozone destruction: The importance of bromine relative to chlorine. *J. Geophys. Res. Atmos.* **1999**, *104*, 23871–23880.
- Salawitch, R. J.; Weisenstein, D. K.; Kovalenko, L. J.; Sioris, C. E.; Wennberg, P. O.; Chance, K.; Ko, M. K.; McLinden, C. A. Sensitivity of ozone to bromine in the lower stratosphere. *Geophys. Res. Lett.* **2005**, *32*, L05811.
- Salawitch, R. J. Atmospheric chemistry: Biogenic bromine. *Nature* **2006**, *439*, 275.
- Badia, A.; Reeves, C. E.; Baker, A.; Volkamer, R.; von Glasow, R. Interactions between volatile organic compounds and reactive halogen in the tropical marine atmosphere using WRF-Chem. *EGU General Assembly Conference Abstracts*, 2016; Vol. 2016.
- von Glasow, R.; Crutzen, P. J. Model study of multiphase DMS oxidation with a focus on halogens. *Atmos. Chem. Phys.* **2004**, *4*, 589–608.
- Charlson, R. J.; Lovelock, J. E.; Andreae, M. O.; Warren, S. G. Oceanic phytoplankton, atmospheric sulphur, cloud albedo and climate. *Nature* **1987**, *326*, 655–661.
- Bates, T. S.; Charlson, R. J.; Gammon, R. H. Evidence for the climatic role of marine biogenic sulphur. *Nature* **1987**, *329*, 319–321.
- Davis, D.; Chen, G.; Bandy, A.; Thornton, D.; Eisele, F.; Mauldin, L.; Tanner, D.; Lenschow, D.; Fuelberg, H.; Huebert, B.; Heath, J.; Clarke, A.; Blake, D. Dimethyl sulfide oxidation in the equatorial Pacific: Comparison of model simulations with field observations for DMS, SO<sub>2</sub>, H<sub>2</sub>SO<sub>4</sub> (g), MSA (g), MS and NSS. *J. Geophys. Res. Atmos.* **1999**, *104*, 5765–5784.

- (31) Malin, G.; Turner, S. M.; Liss, P. S. Sulfur: the plankton/climate connection. *J. Phycol.* **1992**, *28*, 590–597.
- (32) Stefels, J.; Steinke, M.; Turner, S.; Malin, G.; Belviso, S. Environmental constraints on the production and removal of the climatically active gas dimethylsulfide (DMS) and implications for ecosystem modelling. *Biogeochemistry* **2007**, *83*, 245–275.
- (33) Leblanc, C.; Vilter, H.; Fournier, J.-B.; Delage, L.; Potin, P.; Rebuffet, E.; Michel, G.; Solari, P. L.; Feiters, M. C.; Czjzek, M. Vanadium haloperoxidases: From the discovery 30 years ago to X-ray crystallographic and V K-edge absorption spectroscopic studies. *Coord. Chem. Rev.* **2015**, *301–302*, 134–146.
- (34) Manley, S. L.; Barbero, P. E. Physiological constraints on bromoform (CHBr<sub>3</sub>) production by *Ulva lactuca* (Chlorophyta). *Limnol. Oceanogr.* **2001**, *46*, 1392–1399.
- (35) Raina, J.-B.; Clode, P. L.; Cheong, S.; Bougoure, J.; Kilburn, M. R.; Reeder, A.; Forêt, S.; Stat, M.; Beltran, V.; Thomas-Hall, P.; Tapiolas, D.; Motti, C. M.; Gong, B.; Pernice, M.; Marjo, C. E.; Seymour, J. R.; Willis, B. L.; Bourne, D. G. Subcellular tracking reveals the location of dimethylsulfoniopropionate in microalgae and visualises its uptake by marine bacteria. *eLife* **2017**, *6*, No. e23008.
- (36) Curson, A. R. J.; Williams, B. T.; Pinchbeck, B. J.; Sims, L. P.; Martínez, A. B.; Rivera, P. P. L.; Kumaresan, D.; Mercadé, E.; Spurgin, L. G.; Carrión, O.; Moxon, S.; Cattoico, R. A.; Kuzhumpambal, U.; Guagliardo, P.; Clode, P. L.; Raina, J.-B.; Todd, J. D. DSYB catalyses the key step of dimethylsulfoniopropionate biosynthesis in many phytoplankton. *Nat. Microbiol.* **2018**, *3*, 430–439.
- (37) Ansedé, J. H.; Pellechia, P. J.; Yoch, D. C. Nuclear Magnetic Resonance Analysis of [1-<sup>13</sup>C] Dimethylsulfoniopropionate (DMSP) and [1-<sup>13</sup>C] Acrylate Metabolism by a DMSP Lyase-Producing Marine Isolate of the  $\alpha$ -Subclass of Proteobacteria. *Appl. Environ. Microbiol.* **2001**, *67*, 3134–3139.
- (38) Ledyard, K.; Dacey, J. Dimethylsulfide production from dimethylsulfoniopropionate by a marine bacterium. *Mar. Ecol. Prog. Ser.* **1994**, *110*, 95.
- (39) Wolfe, G. V.; Steinke, M. Grazing-activated production of dimethyl sulfide (DMS) by two clones of *Emiliania huxleyi*. *Limnol. Oceanogr.* **1996**, *41*, 1151–1160.
- (40) Steinke, M.; Wolfe, G.; Kirst, G. Partial characterisation of dimethylsulfoniopropionate (DMSP) lyase isozymes in 6 strains of *Emiliania huxleyi*. *Mar. Ecol. Prog. Ser.* **1998**, *175*, 215–225.
- (41) Ansedé, J. H.; Pellechia, P. J.; Yoch, D. C. Metabolism of acrylate to  $\beta$ -hydroxypropionate and its role in dimethylsulfoniopropionate lyase induction by a salt marsh sediment bacterium, *Alcaligenes faecalis* M3A. *Appl. Environ. Microbiol.* **1999**, *65*, 5075–5081.
- (42) De Souza, M. P.; Yoch, D. C. Comparative physiology of dimethyl sulfide production by dimethylsulfoniopropionate lyase in *Pseudomonas douderoffii* and *Alcaligenes* sp. strain M3A. *Appl. Environ. Microbiol.* **1995**, *61*, 3986–3991.
- (43) Stefels, J.; Dijkhuizen, L. Characteristics of DMSP-lyase in *Phaeocystis* sp. (Prymnesiophyceae). *Mar. Ecol. Prog. Ser.* **1996**, *131*, 307–313.
- (44) Stefels, W.; Van Boekel, J. Production of DMS from dissolved DMSP in axenic cultures of the marine phytoplankton species *Phaeocystis* sp. *Mar. Ecol. Prog. Ser.* **1993**, *97*, 11–18.
- (45) Stefels, J. Physiological aspects of the production and conversion of DMSP in marine algae and higher plants. *J. Sea Res.* **2000**, *43*, 183–197.
- (46) Sunda, W.; Kieber, D. J.; Kiene, R. P.; Huntsman, S. An antioxidant function for DMSP and DMS in marine algae. *Nature* **2002**, *418*, 317–320.
- (47) Sunda, W. G.; Hardison, R.; Kiene, R. P.; Bucciarelli, E.; Harada, H. The effect of nitrogen limitation on cellular DMSP and DMS release in marine phytoplankton: climate feedback implications. *Aquat. Sci.* **2007**, *69*, 341–351.
- (48) Vallina, S. M.; Simó, R. Strong relationship between DMS and the solar radiation dose over the global surface ocean. *Science* **2007**, *315*, 506–508.
- (49) Deschaseaux, E. S. M.; Beltran, V. H.; Jones, G. B.; Deseo, M. A.; Swan, H. B.; Harrison, P. L.; Eyre, B. D. Comparative response of DMS and DMSP concentrations in Symbiodinium clades C1 and D1 under thermal stress. *J. Exp. Mar. Biol. Ecol.* **2014**, *459*, 181–189.
- (50) Husband, J. D.; Kiene, R. P.; Sherman, T. D. Oxidation of dimethylsulfoniopropionate (DMSP) in response to oxidative stress in *Spartina alterniflora* and protection of a non-DMSP producing grass by exogenous DMSP+ acrylate. *Environ. Exp. Bot.* **2012**, *79*, 44–48.
- (51) Hughes, C.; Sun, S. Light and brominating activity in two species of marine diatom. *Mar. Chem.* **2016**, *181*, 1–9.
- (52) Mtolera, M. S. P.; Collén, J.; Pedersén, M.; Ekdahl, A.; Abrahamsson, K.; Semesí, A. K. Stress-induced production of volatile halogenated organic compounds in *Eucheuma denticulatum* (Rhodophyta) caused by elevated pH and high light intensities. *Eur. J. Phycol.* **1996**, *31*, 89–95.
- (53) Abrahamsson, K.; Choo, K.-S.; Pedersén, M.; Johansson, G.; Snoeijs, P. Effects of temperature on the production of hydrogen peroxide and volatile halocarbons by brackish-water algae. *Phytochemistry* **2003**, *64*, 725–734.
- (54) Carpenter, L. J.; Archer, S. D.; Beale, R. Ocean-atmosphere trace gas exchange. *Chem. Soc. Rev.* **2012**, *41*, 6473–6506.
- (55) Renirie, R.; Dewilde, A.; Pierlot, C.; Wever, R.; Hober, D.; Aubry, J.-M. Bactericidal and virucidal activity of the alkalophilic P395D/L241V/T343A mutant of vanadium chloroperoxidase. *J. Appl. Microbiol.* **2008**, *105*, 264–270.
- (56) Wolfe, G. V.; Steinke, M.; Kirst, G. O. Grazing-activated chemical defence in a unicellular marine alga. *Nature* **1997**, *387*, 894.
- (57) Sieburth, J. M. Acrylic acid, an “antibiotic” principle in *Phaeocystis* blooms in Antarctic waters. *Science* **1960**, *132*, 676–677.
- (58) Levasseur, M.; Gosselin, M.; Michaud, S. A new source of dimethylsulfide (DMS) for the arctic atmosphere: ice diatoms. *Mar. Biol.* **1994**, *121*, 381–387.
- (59) Asher, E. C.; Dacey, J. W.; Mills, M. M.; Arrigo, K. R.; Tortell, P. D. High concentrations and turnover rates of DMS, DMSP and DMSO in Antarctic sea ice. *Geophys. Res. Lett.* **2011**, *38*, L23609.
- (60) Cota, G. F.; Sturges, W. T. Biogenic bromine production in the Arctic. *Mar. Chem.* **1997**, *56*, 181–192.
- (61) Sturges, W. T.; Cota, G. F.; Buckley, P. T. Bromoform emission from Arctic ice algae. *Nature* **1992**, *358*, 660.
- (62) Müller, E.; von Gunten, U.; Bouchet, S.; Droz, B.; Winkel, L. H. Hypobromous acid as an unaccounted sink for marine dimethyl sulfide? *Environ. Sci. Technol.* **2019**, *53*, 13146.
- (63) Criquet, J.; Rodriguez, E. M.; Allard, S.; Wellauer, S.; Salhi, E.; Joll, C. A.; Von Gunten, U. Reaction of bromine and chlorine with phenolic compounds and natural organic matter extracts—Electrophilic aromatic substitution and oxidation. *Water Res.* **2015**, *85*, 476–486.
- (64) Ossola, R.; Tolu, J.; Clerc, B.; Erickson, P. R.; Winkel, L. H. E.; McNeill, K. Photochemical production of sulfate and methanesulfonic acid from dissolved organic sulfur. *Environ. Sci. Technol.* **2019**, *53*, 13191–13200.
- (65) Liu, Z.-Q.; Shah, A. D.; Salhi, E.; Bolotin, J.; von Gunten, U. Formation of brominated trihalomethanes during chlorination or ozonation of natural organic matter extracts and model compounds in saline water. *Water Res.* **2018**, *143*, 492.
- (66) IHSS (International Humic Substances Society). <http://humic-substances.org/elemental-compositions-and-stable-isotopic-ratios-of-ihss-samples/> (accessed 2021-03-31).
- (67) Önnby, L.; Salhi, E.; McKay, G.; Rosario-Ortiz, F. L.; von Gunten, U. Ozone and chlorine reactions with dissolved organic matter—Assessment of oxidant-reactive moieties by optical measurements and the electron donating capacities. *Water Res.* **2018**, *144*, 64–75.
- (68) Walpen, N.; Schroth, M. H.; Sander, M. Quantification of phenolic antioxidant moieties in dissolved organic matter by flow-injection analysis with electrochemical detection. *Environ. Sci. Technol.* **2016**, *50*, 6423–6432.
- (69) Holland, H. D. *The Chemistry of the Atmosphere and Oceans*; Princeton University Press, 1978; Vol. 1.

(70) Criquet, J.; Allard, S.; Salhi, E.; Joll, C. A.; Heitz, A.; Von Gunten, U. Iodate and iodo-trihalomethane formation during chlorination of iodide-containing waters: Role of bromide. *Environ. Sci. Technol.* **2012**, *46*, 7350–7357.

(71) Feely, R.; Doney, S.; Cooley, S. Ocean acidification: Present conditions and future changes in a high-CO<sub>2</sub> world. *Oceanography* **2009**, *22*, 36–47.

(72) Pinkernell, U.; Nowack, B.; Gallard, H.; Von Gunten, U. Methods for the photometric determination of reactive bromine and chlorine species with ABTS. *Water Res.* **2000**, *34*, 4343–4350.

(73) Ianni, J. C. A comparison of the Bader-Deuffhard and the Cash-Karp Runge-Kutta integrators for the GRI-MECH 3.0 model based on the chemical kinetics code Kintecus. *Computational Fluid and Solid Mechanics 2003*; Elsevier, 2003; pp 1368–1372.

(74) Acero, J. L.; Piriou, P.; Von Gunten, U. Kinetics and mechanisms of formation of bromophenols during drinking water chlorination: Assessment of taste and odor development. *Water Res.* **2005**, *39*, 2979–2993.

(75) Vriens, B.; Mathis, M.; Winkel, L. H. E.; Berg, M. Quantification of volatile-alkylated selenium and sulfur in complex aqueous media using solid-phase microextraction. *J. Chromatogr. A* **2015**, *1407*, 11–20.

(76) Tokarczyk, R.; Moore, R. M. Production of volatile organohalogens by phytoplankton cultures. *Geophys. Res. Lett.* **1994**, *21*, 285–288.

(77) Troy, R. C.; Margerum, D. W. Non-metal redox kinetics: Hypobromite and hypobromous acid reactions with iodide and with sulfite and the hydrolysis of bromosulfate. *Inorg. Chem.* **1991**, *30*, 3538–3543.

(78) Lana, A.; Bell, T.; Simó, R.; Vallina, S.; Ballabrera-Poy, J.; Kettle, A.; Dachs, J.; Bopp, L.; Saltzman, E.; Stefels, J. An updated climatology of surface dimethylsulfide concentrations and emission fluxes in the global ocean. *Global Biogeochem. Cycles* **2011**, *25*, GB1004.

(79) Benner, R.; Pakulski, J. D.; McCarthy, M.; Hedges, J. L.; Hatcher, P. G. Bulk chemical characteristics of dissolved organic matter in the ocean. *Science* **1992**, *255*, 1561–1564.

(80) Spiese, C. E.; Le, T.; Zimmer, R. L.; Kieber, D. J. Dimethylsulfide membrane permeability, cellular concentrations and implications for physiological functions in marine algae. *J. Plankton Res.* **2016**, *38*, 41–54.